Journal of Alloys and Compounds 824 (2020) 153703

Contents lists available at ScienceDirect

Journal of Alloys and Compounds

journal homepage: http://www.elsevier.com/locate/jalcom

Fabrication and assessment of reinforced ceramic electrical insulator from bamboo leaf ash waste

M. Shanmugam [a, *], G. Sivakumar [b], A. Arunkumar [a], D. Rajaraman [c], M. Indhira [d]

[a] Department of Physics, St. Joseph University, Dimapur, 797 115, Nagaland, India
[b] Centralized Instrumentation & Service Laboratory, Annamalai University, Annamalai Nagar, 608 002, Tamilnadu, India
[c] Department of Chemistry, St. Joseph University, Dimapur, 797 115, Nagaland, India
[d] Department of Physics, Vivekanandha College of Arts and Sciences for Women (Autonomous), Tiruchengode, 637 205, India

ARTICLE INFO

Article history:
Received 23 August 2019
Received in revised form
5 December 2019
Accepted 6 January 2020
Available online 7 January 2020

Keywords:
Ceramic electrical insulator
Bamboo leaf ash
Porosity
Flashover

ABSTRACT

This is an attempt to study the effect of bamboo leaf ash (BLA) substitution on quartz in the ceramic insulator sintered at 1250 °C for 2 h. The Physico-mechanical properties, structural, morphological and dielectric characteristics of the ceramic samples were examined by using X-ray diffraction (XRD), Differential thermal analysis (DTA), Transform Infrared spectroscopy (FTIR) and Scanning Electron Microscope (SEM) and dielectric measurement techniques respectively. The study revealed that 10% BLA replacement was better in physico-mechanical performance than the commercial ceramic insulator attributed to the increase of secondary mullite crystals in the BLA reinforced treated sample. Also the incorporation of BLA showed no harmful effect in the ceramic matrix.

© 2020 Elsevier B.V. All rights reserved.

1. Introduction

India holds the second largest bamboo reserve in the world with 10 million hectares of cultivated land. Utilization of bamboo in huge amount is often seen in paper industries with production of large quantity of bamboo leaves as a waste product [1–3]. The waste can be disposed by open firing, and while heating this pyrolysed ash under controlled temperature produces high amount of silica aluminium, iron, and alkalis with trace alkaline earth oxides [4,5]. When heated, this ash under controlled temperature shows an amount of active silica which helps to improve the strength and microstructure of the product. These elements are very important and useful for the partial replacement of the ingredients of cement/ceramic. Currently, the use of agro waste material in ceramic production is a worldwide practice [6]. This utilization protects the environment as well as saves the raw materials for further use in the cement/ceramic industry. The silica present in bamboo have major applications in Pharmacy, Paint industry, Absorbent, Catalyst, Electronic devices such as solar PV cells, semiconductor devices etc. It improves the mechanical strength and stability of the product. Consequently, there is an urgent demand in the development and application of technologies to utilize bamboo leaf ash in the production of ceramic materials from the standpoint of resource and energy conservation as it is cost effective and also helps in reducing CO_2 emission. Efficient utilization of agro forest wastes (BLA) in ceramic industries plays a very significant role in reduction of CO_2 emissions, resources and energy conservation [7]. Although the pyrolysis of bamboo leaves causes CO_2 emission but the amount may not be high as it also improves the ceramic strength as well as saves the raw materials for ceramic production.

The most important application of ceramic materials is to prevent or regulate the flow of current in electrical circuits by being inserted as a barrier between conductors and widely used in the microelectronic devices as well as in power transmission lines [8]. One of the greatest advantages of ceramics as insulators is its high sensitivity even for minor changes in compositions, fabrication techniques, and firing temperatures. According to the literature survey, a limited number of wastes (ashes) such as fly ash [9], rice husk ash [10] and sugarcane bagasse ash [11] are utilized as an additive to produce ceramic materials. To the best of our knowledge, no report is found in the replacement of ceramic ingredient like quartz by bamboo leaf ash (BLA) and a very limited report on the dielectric behavior of forest waste based ceramic materials. Hence, the objective of this work is to study the effect of BLA concentrations on the partial and whole replacement of quartz in

* Corresponding author. Tel.: +91 9688268895.
E-mail address: shanmuga2131@gmail.com (M. Shanmugam).

https://doi.org/10.1016/j.jallcom.2020.153703
0925-8388/© 2020 Elsevier B.V. All rights reserved.

ceramic electrical insulator through XRD, SEM, and dielectric measurement techniques and comparison of physico-mechanical test results.

2. Experimental design

2.1. Preparation of raw materials

The standard ceramic ingredients (clay, feldspar and quartz) were purchased from M/s Oriental Ceramic Industry, Viruthachalam, Cuddalore district, Tamil Nadu. The bamboo leaf ash processing as described by Alaneme et al. (2014). Initially, the collected bamboo leaves were washed thoroughly with tap water to remove the dirt and earthen materials. The leaves were dried in the sun light for 12 h and cut into small pieces for firing in the open air to allow complete combustion. Then the produced ash (black ash) was allowed to cool in an open environment for 24 h and dried at 110 °C in a hot air oven for 1 h. Then grained and sieving ash was calcined at 650 °C for 3 h in a muffle furnace in the ambient atmosphere, the milky white coloured powder was obtained and it replaces the quartz [12].

2.2. Fabrication of ceramic insulator

Standard ceramic (SC) and BLA reinforced ceramic insulators were fabricated according to the standard procedure ASTM C373 by using ceramic ingredients, such as clay, feldspar, quartz and BLA. Table 1 shows the batch composition of experimental ceramic insulators. For the fabrication of SC, the dried ceramic ingredient powder was thoroughly mixed to obtain a homogeneous mixture by a mini ball mill using GRACE Digital Timer (Stainless steel ball mill) GKBM-5 (80 rpm speed). Then adequate (6–7%) distilled water was added to the powder for adhesion and then the slurry was milled to ensure homogeneity for 12 h.

Consequently, the slip was pressed using a manual hydraulic uniaxial press and a steel matrix (32 mm × 16 mm X 3 mm) Fig. 1 to handle four samples simultaneously. The moisture content in the system was adjusted to 4–5% [13] for attaining smooth surface of the product and then dried for 48 h. Then the dried (green) ceramic insulator was sintered under the controlled temperature of 1250 °C for 2 h by using an electric kiln with a heating and cooling rate of 6 °C/min at room temperature. A similar procedure was adopted for the preparation of BLA reinforced ceramic electrical insulators. Quartz was replaced in standard ceramic by 5, 10, and 15 wt% of calcined ash (650 °C). The photograph of fabricated specimens is shown in Fig. 2 which seems to be typical commercial ceramic product.

2.3. Characterization techniques

Physical tests such as water absorption (WA), porosity (P) and bulk density (BD) of the sintered specimens were carried out according to Archimedes principle (ASTM test method (20–83, 493-70). The mechanical strength (MS) was measured by using a universal testing machine. Crystalline phases in the ceramic matrix were analysed by using X-ray diffraction (D/Max ULTIMA) patterns.

Table 1
Batch composition (wt %) of the experimental ceramic insulators.

Specimens	Clay	Feldspar	Quartz	BLA
SC	60	25	15	0
QB1	60	25	10	5
QB2	60	25	05	10
QB3	60	25	00	15

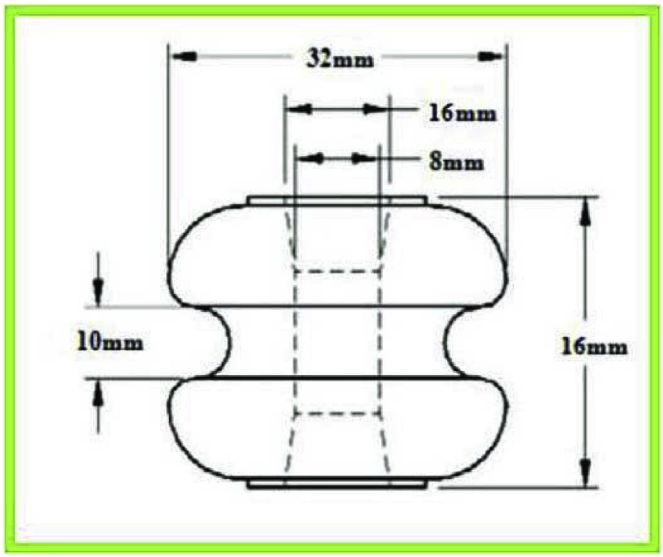

Fig. 1. Block diagram of ceramic insulator.

Fig. 2. Standard and experimental ceramic insulator.

The functional groups present in the specimens were identified from the Fourier Transform Infra Red (FT-IR) spectra recorded in the range of 4000 to 400 cm^{-1} by Perkin Elmer FTIR spectrometer (Model RX-1) with the resolution of ±4 cm^{-1}. Microstructures of the specimens were observed by JEOL-JSM 5610 LV- Scanning Electron Microscope under the magnification of 1000 and 10,000 eV.

Differential thermal analysis (TG/DTA) of the waste sample was performed in a temperature range of 25–1500 °C, using Thermal analyser NETZSCH-STA44F3 JUPITER with a heating rate 20 °C/mm under the nitrogen gas atmosphere. Dielectric properties of the specimens were carried out using standard test methods for flashover voltage of solid insulating material (ASTM D149).

3. Results and discussion

3.1. Chemical composition of BLA

Table 2 displayed the chemical composition of BLA that contains a large amount of silica (79.90%), and the lesser amount of alumina (Al_2O_3), calcium oxide (CaO), iron oxide (Fe_2O_3) and potassium oxide (K_2O). The chemical composition of the BLA was analysed by X-ray Fluorescence (Bruker).

3.2. Thermal analysis of BLA

Fig. 3 shows the TG/DTA curves of raw pristine bamboo leaf ash (Room temperature to 1000 °C). By this technique, the oxidation

Table 2
Chemical composition of the raw materials (wt %).

Composition	Clay	Feldspar	Quartz	BLA
SiO_2	63.45	64.20	97.55	79.90
Al_2O_3	29.33	14.02	0.97	2.78
Fe_2O_3	3.17	0.38	0.27	0.86
K_2O	1.15	16.83	0.41	3.98
CaO	0.33	0.65	0.23	7.84
MgO	0.39	0.28	0.08	1.97
Na_2O	0.28	2.90	0.35	0.20
TiO_2	1.57	0.35	0.04	0.38
Others	0.66	0.26	0.10	2.09

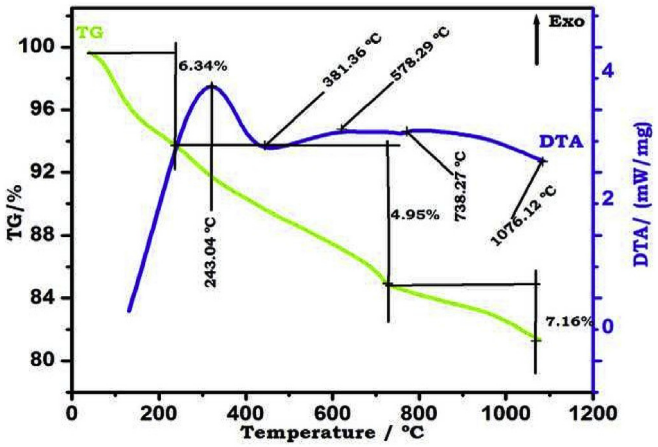

Fig. 3. TG/DTA curves of pristine bamboo leaf ash.

behaviour of the samples is investigated, and the temperature at which all remaining carbon fully burnt is exactly determined. The different steps of weight loss occur at the heating rate of 20 °C/min as shown in the thermograms (TG). From the start of the experiment (room temperature) to 250 °C, the amount of weight loss is (~6.34%) recorded. The initial loss is attributed to the evaporation of moisture from the sample and the external water bound. It is important to notice that second part of the mass loss (4.95%) was observed in the range of 250–700 °C, which belongs to organic compounds volatilization and oxidation. The small exothermic peak around 250–400 °C, correspond to the volatile matter which is due to the decomposition of the three major bamboo leaf components such as cellulose, hemicellulose and lignin. The combustion of these volatile substances also dehydrates the calcium phosphate content [14].

The ash with the thermal patterns (700–1000 °C) in the weight loss (third step) probability (7.16%) shows the presence of some aluminium silicate from the other mineral family and the characteristic peak of α→β quartz transformation confirms the predominance of this crystalline silicate in BLA.

It is clearly revealed from the Table 2, that the BLA contains a large amount of silica (~80%), from the XRD analysis (Fig. 4), hexagonal structure of quartz is the dominant phase in comparison to cristobalite. When temperature is applied to BLA, α-quartz phase (up to 600 °C) transition to β-Quartz (600 °C–800 °C) takes place. The phase change influenced the thermal stability of the BLA and modifies the physical-mechanical behavior of the system.

The endothermic peak around ~381 °C is may be due to the decomposition of cellulosic part and bonding of organic molecules with silicon in bamboo leaf ash. During the temperature range between 200 and 500 °C, the removal of volatile matter makes pore opening and many pores with the rough surface and the irregular

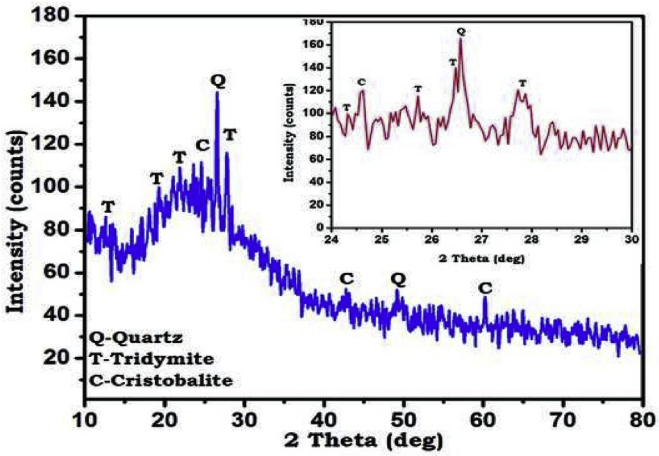

Fig. 4. XRD pattern of bamboo leaf ash.

outlets are created, leading to a significant increase in surface area and porosity. An exothermic peak appears in the DTA curve (738.27 °C) corresponds to the crystallization of the existing metaphase (crystalline SiO_2) [15]. The exothermic reaction is mainly caused by the re-crystallization on new phases. This exothermic reaction is attributed mainly due to the thermal decomposition and oxidation of organic compounds (charcoal and organic matter) [16].

3.3. Powder XRD analysis of BLA

The observation of powder X-ray diffraction analysis of the BLA (calcined at 650 °C) at room temperature is shown in Fig. 4. The diffraction pattern shows a broad hump around $2\theta = 15–35°$ owing to partially crystalline silica. Peaks obtained around $2\theta = 26.63°$ belongs to (0 1 1) and a weak reflection at $2\theta = 49.95°$ belongs to (1 1 2) plane of hexagonal structure of quartz (SiO_2) (JCPDS card no. 85–1780), cristobalite (SiO_2) peak at $2\theta = 42.76°$ and 60.45° (JCPDS No. 89–3434). In addition to the above, peaks around $2\theta = 12.69°$, 19.36°, 27.39° belongs to (0 2 6), (1 3 7) and (2 4 0) which are in agreement with the JCPDS card no. 71–0261 [17].

This is in consistent with the powder XRD results. A strong exothermic event was observed at the temperature range of 500–700 °C. The XRD analysis confirms the presence of quartz (SiO_2) in the calcined ash at 650 °C while in the case of TG/DTA analysis, α-β quartz transition and crystallization of silica is identified. The XRD data for calcined BLA was recorded at the temperature range of 650 °C.

3.4. Physical and mechanical properties-

Physical properties such as water absorption (WA) and porosity (P), Bulk density (BD) and mechanical strength (MS) of the sintered specimens were carried out according to Archimedes principle ASTM test method (20–83, 493–70 and C373-88). Fig. 5 shows the porosity and water absorption results of the standard and BLA reinforced ceramic electrical insulators.

3.4.1. Porosity (P)

Porosity was calculated as a function of the specimens weight differences between saturated weight (W_{sat}) and dry weight (W_d) to the weight difference between saturated and suspended weight (W_{sus}). The porosity can be calculated by using the relation

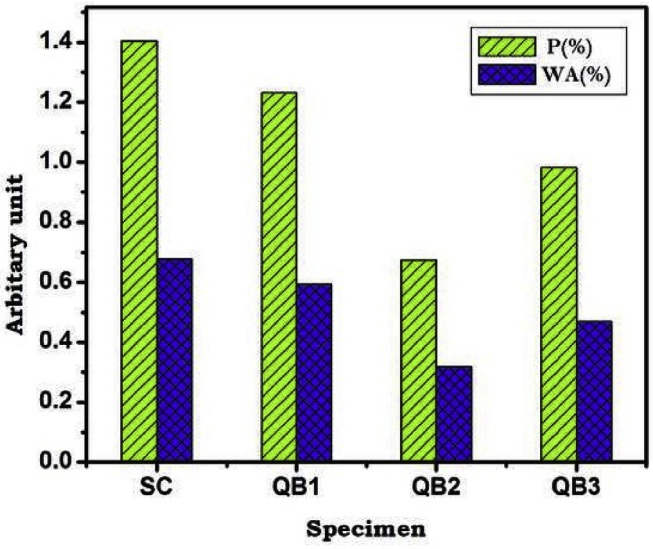

Fig. 5. Physical properties: porosity (P), Water absorption (WA) of the experimental ceramic insulator.

$$\text{Porosity(P)} = \frac{W_{sat} - W_d}{W_{sat} - W_{sus}} \times 100\ (\%)$$

It is noticed that the percentage porosity of standard insulator (1.4052%) is higher as twice in comparison to QB1 (1.2319%), QB2 (0.6757%) and QB3 (0.9823%). It is the fact that the replacement of quartz by active silica (microfiller) in BLA decreases porosity and influence to the densification of the ceramic matrix. Hence, the higher BLA incorporated ceramic insulator (QB2 and QB3) showed less than 1% porosity due to decrease in apparent porosity with BLA content. The results indicate that the fabricated ceramic insulators are more vitrified than the standard ceramic insulator.

3.4.2. Water absorption (WA)

Water absorption was calculated as a function of the specimens weight difference prior to and after water submersion. Dry ceramic specimen with pores will gain weight by immersion in water. The amount of water absorbed is the measure of porosity obtained, however, varies considerably with a method of immersion, i.e., time and temperature [18]. It expresses the relationship between the mass of water absorbed into the mass of the dry specimens as follows:

$$\text{Water Absorption (WA)} = \frac{W_{sat} - Wd}{W_d} \times 100\ (\%)$$

The results indicated that the water absorption of BLA reinforced ceramic insulators are lower value (0.3189 for 10%, 0.4698% for 15% and 0.5932% for 5% BLA) when compared to the standard ceramic insulator (0.6784%). This can be accredited to the active silica particles filled in pores.

3.4.3. Bulk density (BD)

Fig. 6 shows the bulk density and mechanical strength results of the standard and BLA reinforced ceramic electrical insulators. Bulk density is calculated by using the relation as given below,

$$\text{Bulk density(BD)} = \frac{W_d}{W_{sat} - W_{sus}} \times \text{Density of water}\left(g \Big/ cm^3\right)$$

It is observed that the bulk density of the SC is found to be 2.0503 g/cm^3 and it is enhanced in the case of BLA incorporated ceramic matrix. It is found about 2.0546 (g/cm^3), 2.1034 (g/cm^3) and 2.0712 (g/cm^3) respectively for 5%, 10% and 15% BLA. The restoration of BLA incorporated ceramic insulators are due to active silica present in BLA that close porous as well as high shrinkage (ie) the binding particles to form the denser media.

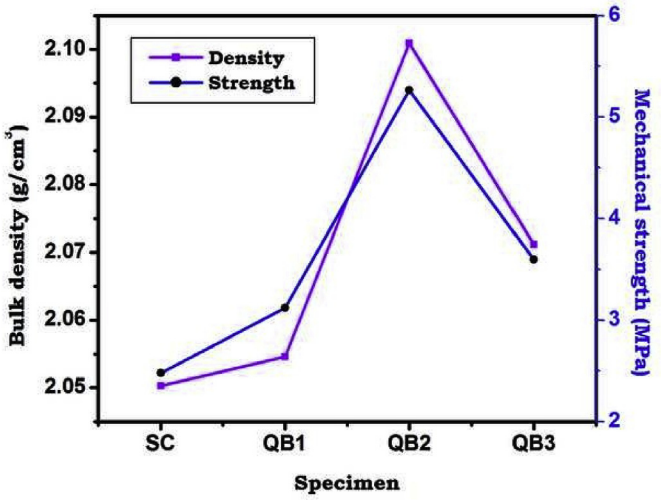

Fig. 6. Strength and density of the experimental ceramic insulator.

3.4.4. Mechanical strength (MS)

The mechanical strength of the ceramic insulators was recorded by using a universal testing machine (UTM). The BLA reinforced ceramic insulators have exhibited better mechanical strength than the standard ceramic insulator (2.48 MPa). The mechanical strength values are found to be 3.12, 5.265 and 3.595 MPa for 5%, 10% and 15% BLA respectively [19]. The increase of mechanical strength with respect to BLA content is attributed to dispersion-strengthening effect, because the BLA act as dispersal solids in the glassy matrix.

The result is related to the improvement in granular size distribution and significantly closes the pores which results in shrinkage causing dense structure of BLA reinforced ceramic insulator. Besides it's better physical and mechanical strength, the results shown in BLA ceramic insulators are due to the presence of active silica which leads to high densification in the ceramic matrix. The test results have proved that the BLA identified as the potential ceramic ingredient are for the feature ceramic resource material.

3.5. Dry power frequency flashover voltage

The dry power frequency flashover voltage measurement for the experimental ceramic insulator is shown in Fig. 7. The test was conducted according to ANSI C29-1&3 procedures (Olupot, 2010). An alternating current of 50 Hz frequency was applied to the test specimen in air and the voltage was quickly raised to the constant value of 2 kV/s (1/50 μs waves) and rise slowly until a flashover occurs.

The recorded flashover voltage value was the arithmetic mean of three individuals (reel type cylindrical ceramic electrical insulator). The period values for flashovers were between 30 s and 3 min in air at room temperature. The flashover voltage is the highest value if the field strength can be applied to an insulating material just before the breakdown occurs. The total breakdown voltage is determined by placing electrodes on opposite surfaces of a specimen disc (experimental ceramic insulator) and increasing

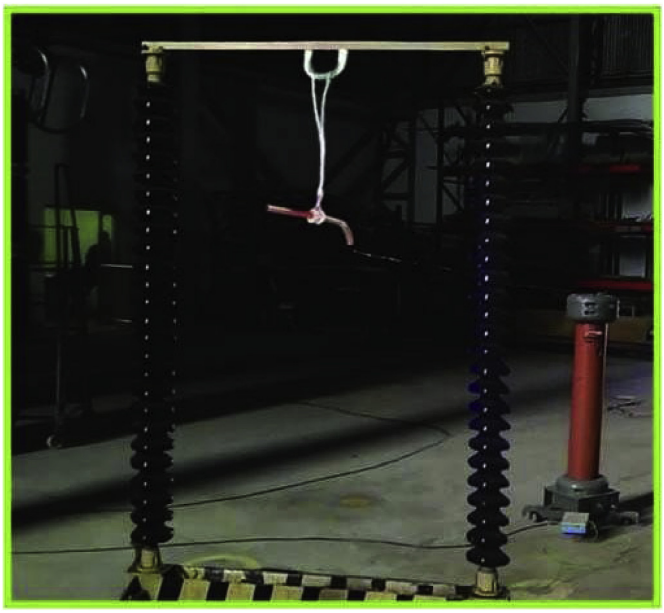

Fig. 7. Dielectric flashover voltage measurement setup.

the potential difference between the electrodes until the material cannot resist the flow of current [20]. The flashover voltage of the BLA reinforced ceramic electrical insulators is found to be higher, about 9.22 kV/mm, 10.40 kV/mm and 9.91 kV/mm for QB, QB2 and QB3 respectively than that of SC (8.65 kV/mm).

3.6. XRD analysis

Fig. 8 shows the XRD patterns of the SC and BLA reinforced ceramic insulator that indicates the crystalline quartz (SiO_2) at $2\theta = 26.61°$ (011) and mullite ($3Al_2O_3 \cdot 2SiO_2$) at $2\theta = 35.27°$ (111), 40.87° (121) and 60.71° (331). These results agree well with the standard JCPDS card no 898935 and 150776. It is an important notice that the intensity of mullite peaks gets increased while decreasing the crystalline quartz peaks with respect to BLA content. The crystalline peaks are seen in BLA reinforced specimens at $2\theta = 54.04°$ (420) and 57.60° (041) (JCPDS. No. 791458) belong to secondary mullite ($2Al_2O_3 \cdot 2SiO_2$). It is the result of the reaction between melt and clay relics. The BLA particles adhere well to the kaolin particles to form metakolinites under controlled sintering and finally it transformed to mullite [21–23]. The intensity of secondary mullite peaks are found better in 10% BLA reinforced sample than remaining concentrations. Note that this product is responsible for the strength of the sample. The result suggests that 10% BLA reinforced ceramic attained better mechanical properties due to crystallization of mullite and reduction of quartz contents. Crystallite size of powder XRD pattern was measured using line Debye Scherer formula described by sultana et al. (2011) and found to be 11–62 nm range.

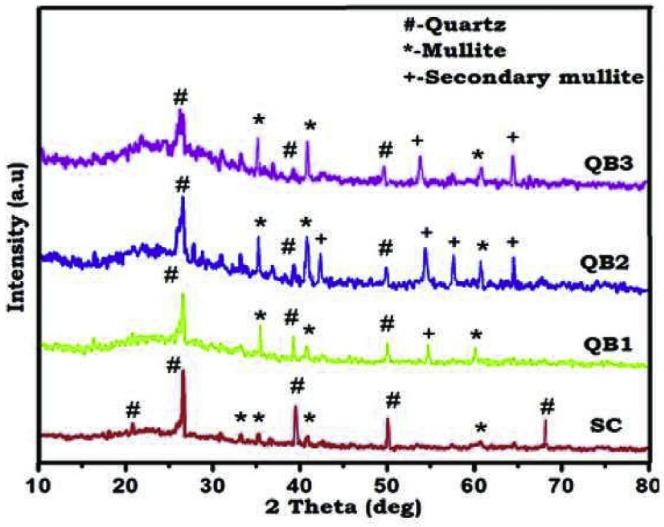

Fig. 8. XRD patterns of the experimental ceramic insulator.

3.7. FTIR analysis

The FTIR spectra of standard and BLA reinforced ceramic electrical insulators are shown in Fig. 9. By comparing the vibrational spectra, the BLA reinforced ceramic insulators seem to be similar to that of SC insulator. However, the intensity of asymmetric stretching vibration of quartz (Si–O–Si) band (1070-1095 cm^{-1}) gets decreased while the mullite (Si–O– Al) peaks (at 788 cm^{-1} and 540 cm^{-1}) get broadened by increasing the BLA content.

It might be the fact that either the mullite vibration of crystallites or the feature is consistent with superposition of Si–O vibrations in the SiO_4 tetrahedral [24,25] of sintered specimen. The FTIR analysis confirms the presence of mullite and quartz phases in the ceramic insulators that support the XRD results.

3.8. Microstructural analysis

A thin layer of fractured surface of samples has been stubbed using the double-sided carbon tape. Samples are coated with the help of gold coater (JEOL Auto fine coater, model JFS- 1600). Coating time is 120 s with 20 mA and with an accelerating voltage of 20 kV at high vacuum mode.

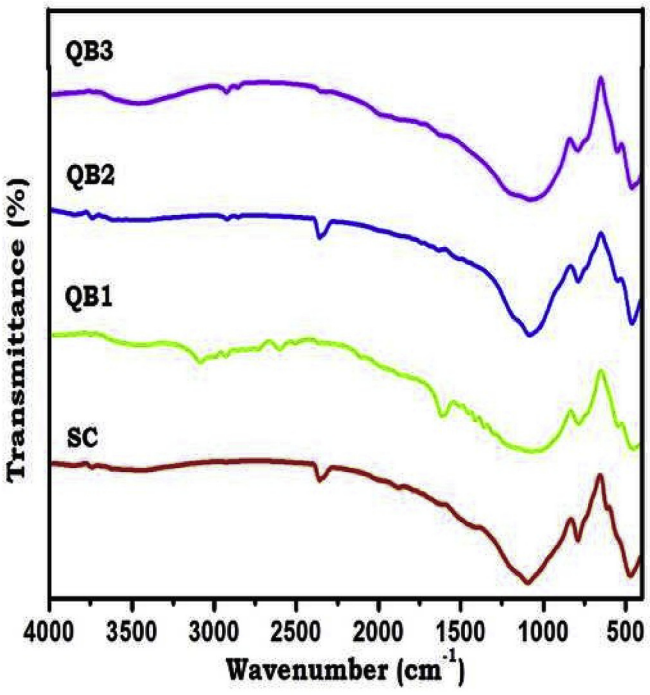

Fig. 9. FTIR analysis of the experimental ceramic insulator.

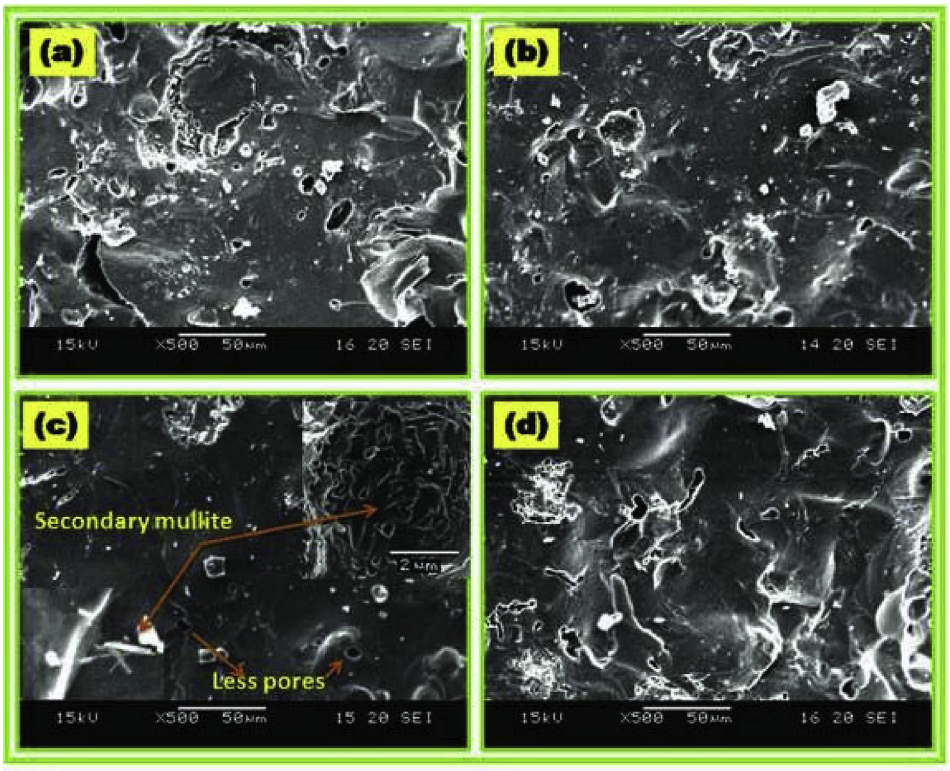

Fig. 10. SEM micrographs of the experimental ceramic insulator (a) SC, (b) QB1, (c) QB2, (d) QB3.

The microstructure of the sintered specimen (1250 °C) SC shows open pores on the texture and not -homogenous surface is shown in Fig. 10a. It could be attributed to the removal of volatile matter which makes a pore opening and pores with the rough surface and irregular outlet is created, leading to a significant increase in surface area and porosity. The average pore size is found nearly 5 μm. By comparing the SEM images of BLA ceramic insulators, with the standard ceramic insulator (SC) the size of the pores are minimized in QB1 (5%) (Fig. 10b) and pores are not seen in the QB2 (10% BLA) reinforced ceramic electrical insulator (Fig. 10c). Fine needle-shaped mullite crystals are higher in the 10% BLA specimen [26–28].

In the case of the 15% BLA reinforced ceramic insulator (Fig. 10d), a number of coarse particles, irregularly shaped pores and lower amount of mullite crystals are seen. The SEM analysis of 10% BLA reinforced ceramic insulator has the compact glassy matrix with fine secondary mullite crystals. The results are in agreement with physical and mechanical strength values.

4. Conclusions

The following conclusions can be drawn from the results and discussion obtained herein.

The BLA waste used in this study is a zero cost material that can replace natural quartz in the processing of reinforced ceramic electrical insulator formulations was investigated. Aside from the environmental and economic benefits of sinking BLA waste, the replacement of up to 10 wt% BLA waste with quartz allows for the fabrication of reinforced insulator sintered controlled temperature 1250 °C.

The results obtained in physical and mechanical tests like shrinkage, porosity, water absorption, bulk density, and mechanical strength have good and improved the reinforced ceramic insulator by replacement of quartz with up to 10 wt% BLA waste. XRD analysis showed that reinforced ceramic electrical insulator produced was formed primarily by three components: quartz, mullite, and the needle-shaped crystals of mullite in the polished network were identified. SEM observations indicated that the reinforced insulators were acclimated as quartz diminished and increased mullite in the 10% BLA substitution. The dielectric flashover voltage was likewise upgraded for the 10% BLA strengthened exploratory encasing contrasted with different specimens which were expected with higher mullite crystallite size.

The management of BLA waste by incorporation into reinforced insulator is rather promising and has the potential to minimize the waste generated from the bamboo forest.

Author Contribution statement

Shanmugam Marimuthu: Methodology, Software, Writing-Original draft preparation, Visualization, Investigation.
Sivakumar Ganesan: Supervision, Validation.
Arunkumar Arumugam: Writing- Reviewing and Editing

Declaration of competing interest

The authors declare that they have no known competing financial interests or personal relationships that could have appeared to influence the work reported in this paper.

Acknowledgement

The authors are grateful to Mr. Parthasarathy, Managing Director, M/s Orient Ceramic Industry, Virudhachalam for providing the ceramic materials and sincere gratitude to Mr. V. Pandiyan, Deputy General Manager, M/s Global Power Research Institute,

Kurinchipadi for dielectric flashovers measurement.

References

[1] Sankar Mohapatra, R. Sakthivel, G.S. Roy, Shikha Varma, S.K. Singh, Dilip Kumar Mishra, Synthesis of-SiC powder from bamboo leaf in a DC extended thermal plasma reactor, Mater. Manuf. Process. 26 (2011) 1362–1368, https://doi.org/10.1080/10426914.2011.557127.

[2] Shi-jian Yang, Mei Sun, Yong-jiang Zhang, Hereve Cochard, Kun Fang Cao, Strong leaf morphological, anatomical, and physiological responses of a subtropical woody bamboo (Sinarundinaria nitida) to contrasting light environments, Plant Ecol. 215 (1) (2014) 97–109.

[3] Moisés Fríasa, Holmer Savastano, Ernesto Villar, M. Isabel Sánchez de Rojas, Sergio Santos, Characterization and properties of reinforced cement matrices containing activated bamboo leaf wastes, Cement Concr. Compos. 34 (2012) 1019–1023.

[4] Ernesto Villar-Cociña, Eduardo Valencia Morales, Sergio F. Santos, Holmer Savastano Jr., Moisés Frías, Pozzolanic behaviour of bamboo leaf ash: characterization and determination of the kinetic parameters, Cement Concr. Compos. 33 (2011) 68–73.

[5] K. Amutha, G. Sivakumar, Analytical analysis of synthesized biosilica from bioresidues, Spectrochim. Acta A Mol. Biomol. Spectrosc. 112 (2013) 219–222.

[6] Y. Dong, X. Feng, X. Feng, Y. Ding, Preparation of low-cost mullite ceramics from natural bauxite and industrial waste fly ash, J. Alloy. Comp. 460 (1–2) (2008) 599–606, https://doi.org/10.1016/j.jallcom.2007.06.023, 2008.

[7] T. Zhang, P. Gao, P. Gao, J. Wei, Q. Yu, Effectiveness of novel and traditional methods to incorporate industrial wastes in Cementitious materials- an overview, Resour. Conserv. Recycl. 74 (2013) 134–143, https://doi.org/10.1016/j.resconrec.2013.03.003.

[8] S. Nagata, H. Katsui, K. Hoshi, B. Tsuchiya, K. Tohc, M. Zhaoa, T. Shikamaa, E.R. Hodgson, Recent research activities on functional ceramics for insulator, breeder and optical sensing systems in fusion reactors, J. Nucl. Instrum. Methods Phys. Res. B J. Nuc. Mater. 442 (2013) S501–S507.

[9] Z. Jing, Y.-Y. Li, S. Cao, Y. Liu, Performance of double-layer biofilter packed with coal fly ash ceramic granules in treating highly polluted river water, Bioresour. Technol. 120 (2012) 212–217, https://doi.org/10.1016/j.biortech.2012.06.069.

[10] S.V. Vassilev, D. Baxter, L.K. Andersen, C.G. Vassileva, T.J. Morgan, An overview of the organic and inorganic phase composition of biomass, Fuel 94 (2012) 1–33.

[11] S. Wattanasiriwech, D. Wattanasiriwech, J. Svasti, Production of amorphous silica nanoparticles from rice straw with microbial hydrolysis pretreatment, J. Non-Cryst. Solids 356 (2010) 1228–1232.

[12] K.K. Alaneme, P.A. Olubambi, A.S. Afolabi, M.O. Bodurin, Corrosion and tribological studies of bamboo leaf ash and alumina reinforced Al-Mg-Si alloy matrix hybrid composites in chloride medium, Int. J. Electrochem. Sci. 9 (2014) 5663–5674.

[13] A. E Souza, S.R. Texieria, G.T. a Santos, F. B Costa, e. Longo, Reuse of sugarcane Bahasse ash (SCBA) to produce ceramic materials, J. Environ. Manag. 92 (2011) 2774–2780.

[14] Peter W. Olupot, Stefan Jonsson, Joseph K. Byaruhanga, Effects of the sintering process on properties of triaxial electrical porcelain from Ugandan ceramic minerals, World Acad. Sci. Eng. Technol. 77 (2013), 05-20.

[15] K.C.P. Faria, R.F. Gurgel, J.N.F. Holanda, Recycling of sugarcane bagasse ash waste in the production of clay bricks, J. Environ. Manag. 101 (2012) 7–12.

[16] Y. Meng, G. Gong, Z. Wu, Z. Yin, Y. Xie, S. Liu, Fabrication and microstructure investigation of ultra-high-strength porcelain insulator, J. Eur. Ceram. Soc. 32 (12) (2012) 3043–3049, https://doi.org/10.1016/j.jeurceramsoc.2012.04.015.

[17] J. Martin-Marquez, J. Ma Rincon, M. Romero, Effect of firing temperature on sintering of porcelain stoneware tiles, Ceram. Int. 34 (2008) 1867–1873.

[18] S. Wattanasiriwech, D. Wattanasiriwech, J. Svasti, Production of amorphous silica nanoparticles from rice straw with microbial hydrolysis pretreatment, J. Non-Cryst. Solids 356 (2010) 1228–1232.

[19] Benneth C. Chukwudi1, Patrick O. Ademusuru, Boniface A. Okorie, Characterization of sintered ceramic tiles produced from steel slag, J. Miner. Mater. Charact. Eng. 11 (2012) 863–868.

[20] Nana Xu, Shujing Li, Yuanbing Li, Zhengliang Xue, Lin Yuan, Jinlong Zhang, Lei Wang, Preparation and properties of porous ceramic aggregates using electrical insulator waste, Ceram. Int. 41 (4) (2015) 5807–5811, https://doi.org/10.1016/J.Ceramint.2015.01.009.

[21] M. Ehsania, H. Borsi, E. Gockenbach, J. Morshedian, G.R. Bakhshandeh, An investigation of dynamic mechanical, thermal, and electrical properties of housing materials for outdoor polymeric insulators, Eur. Polym. J. 40 (2004) 2495–2503.

[22] T.K. Mukhopadhyay, S. Ghosh, J. Ghosh, S. Ghatak, H.S. Maiti, Effect of fly ash on the physico-chemical and mechanical properties of a porcelain composition, Ceram. Int. 36 (2010) 1055–1062.

[23] P. Sultana, S. Das, B. Bagchi, A. Bhattacharya, R. Basu, P. Nandy, Effect of size of fly ash particle on enhancement of mullite content and glass formation, Bull. Mater. 34 (7) (2011) 1663–1670.

[24] R. Palanivel, G. Velraj, FTIR and FT-Raman spectroscopic studies of fired clay artifacts recently excavated in Tamilnadu, Int. J. Pure Appl. Phys. 45 (2007) 501–508.

[25] W. Wang, H.LiY. Guo, q. sun, Chen, Mullite whiskers prepared by molten salt method using Si powders, J. Adv. Ceram. 4 (2013) 283–289.

[26] Kausik Dana, Swapan kumar Das, Evolution of microstructure in fly ash-containing porcelain body on heating at different temperatures, Bull. Mater. Sci. 27 (2) (2004) 183–188.

[27] Y. Meng, G. Gong, D. Wei, Y. Xie, Z. Yin, Comparative microstructure study of high strength alumina and bauxite insulator, Ceram. Int. 40 (2014) 10677–10684.

[28] Muthafar F. Al-Hilli, Kalid T. Al-Rasoul, Influence of glass addition and sintering temperature on the structure, mechanical properties and dielectric strength of high-voltage insulators, Mater. Des. 31–38 (2010) 85–3890.